Volume 13 Number 13 1985 Nucleic Acids Research

Molecular recognition of B-DNA by Hoechst 33258+

Keith D.Harshman and Peter B.Dervan*

Division of Chemistry and Chemical Engineering, California Institute of Technology, Pasadena, CA 91125, USA

Received 18 March 1985; Revised and Accepted 27 May 1985

ABSTRACT

The binding sites of Hoechst 33258, netropsin and distamycin on three DNA restriction fragments from plasmid pBR322 were compared by footprinting with methidiumpropyl-EDTA·Fe(II) [MPE·Fe(II)]. Hoechst, netropsin and distamycin share common binding sites that are five ± one bp in size and rich in A·T DNA base pairs. The five base pair protection patterns for Hoechst may result from a central three base pair recognition site bound by two bisbenzimidazole NHs forming a bridge on the floor of the minor groove between adjacent adenine N3 and thymine O2 atoms on opposite helix strands. Hydrophobic interaction of the flanking phenol and N-methylpiperazine rings would afford a steric blockade of one additional base pair on each side.

INTRODUCTION

Hoechst dye 33258 (H) is a bisbenzimidazole that binds double helical DNA rich in adenine (A) and thymine (T) base pairs (1-2). Martin and Holmes have shown that the binding of Hoechst 33258 on DNA requires a minimum of four consecutive A·T base pairs (2). Hoechst is of similar size and shape to the di- and tripeptides, netropsin and distamycin, which show a marked preference for A·T rich DNA (3-13). From a recent X-ray analysis of the complex of netropsin with the B-DNA dodecamer of sequence CGCGAATTCGCG, Dickerson and coworkers provide a molecular basis for the sequence specific recognition of DNA by netropsin, and, by extension, distamycin (14). They find that the crescent shaped netropsin sits symmetrically in the center of the minor groove of right-handed DNA and displaces the water molecules of the spine of the hydration (14). Each of its three amide NH groups forms a bridge between adjacent adenine N3 or thymine O2 atoms on opposite helix strands (14). This explains recent data that distamycin-like analogues having n-amides characteristically bind to n+1 successive base pairs (15-17). The inside edge of the crescent framework of Hoechst has potential NH recogniton elements similar in disposition in space to the carboxamide NHs of netropsin and distamycin. Mikhailov and coworkers have suggested that the bisbenzimidazole framework of Hoechst forms a helix isogeometric to B-form DNA similar to netropsin and distamycin (1). A crystal structure of Hoechst dye bound to DNA does not yet exist. However, with the availability of the netropsin:DNA dodecamer crystal structure (14), it

would seem appropriate to ask by footprinting methods whether Hoechst, netropsin, and distamycin, molecules similar in shape though different in chemical structure, share common binding sites on B-form DNA. Accurate resolution of the binding site sizes may provide insight on the number of hydrophobic, hydrogen bonding, and electrostatic recognition elements for each molecule. We report here a comparison of the binding sites of Hoechst 33258, netropsin, and distamycin on three ^{32}P end-labeled restriction fragments from plasmid pBR322 by footprinting methods. We use the synthetic DNA cleaving agent, methidiumpropyl-EDTA·Fe(II) (MPE·Fe(II)) which has been shown to resolve binding site sizes more accurately than the enzyme DNase I (18-19).

MATERIALS AND METHODS

Reagents and Enzymes. Distamycin A was obtained from Boehringer Mannheim. Hoechst dye 33258 was obtained from Calbiochem. Netropsin was a gift of D. Patel. Methidiumpropyl-EDTA (MPE) was synthesized and purified as described by Hertzberg and Dervan (20-21). Purities were determined by thin layer chromatography. Concentrations were determined spectroscopically. Dithiothreitol (DTT) was obtained from Calbiochem. Ferrous ammonium sulfate, $Fe(NH_4)_2(SO_4)_2 \cdot 6\ H_2O$ was obtained from Baker. Restriction endonucleases and the Klenow fragment of DNA polymerase I were obtained from New England Biolabs. Bacterial alkaline phosphatase and T4 kinase were obtained from BRL.

DNA Restriction Fragments. Three restriction fragments from plasmid pBR322 were prepared. Superhelical plasmid pBR322 was first digested with restriction endonuclease Bam H1 and labeled at the 3'-end with α-^{32}P dATP and the Klenow fragment of DNA polymerase I. A second enzymatic digest with Eco RI yielded the 3' end-labeled 381 bp fragment which was isolated according to the procedures of Maxam-Gilbert (21). The 5' end-labeled 381 bp fragment was obtained by treatment of Bam H1 digested plasmid pBR322 first with bacterial alkaline phosphatase and then with γ-^{32}P ATP and T4 kinase prior to restriction with Eco RI. The plasmid pBR322 was labeled at the 5' and 3' end at the Eco RI site, followed by restriction with Rsa I to yield the end-labeled 167 and 517 bp fragments.

Footprinting. The MPE·Fe(II) cleavage reactions were run in a buffer (TN) containing 10 mM Tris, pH 7.4 and 50 mM NaCl. To 4 µL solution containing 2.5 x TN buffer, >600 cpm ^{32}P end-labeled restriction fragment, and 250 µM (base pair) sonicated calf thymus DNA was added 2 µL of the inhibiting compound of the appropriate concentration (see Fig. 2 for final concentrations). This solution was incubated in the dark for 30 min at 37°C. Next, 2 µL of a freshly prepared solution containing 12.5 µM MPE and 25 µM $Fe(NH_4)_2(SO_4)_2$ was added. This was incubated for an additional 15 min at 37°C. The cleavage reaction was initiated by the addition of 2 µL freshly prepared 20 mM dithiothreitol, bringing the total reaction volume to 10 µL. The cleavage reaction was allowed to continue for 15 min at 37°C before stopping by freezing in dry ice. The

samples were then lyopholyzed and resuspended in 4 µL of formamide loading buffer.

Sequencing Gels. Cleavage inhibition patterns were determined by electrophoresis on 0.4 mm thick, 40 cm long, 8% polyacrylamide (167 and 517 bp fragments) or 5% polyacrylamide (381 bp fragment), 1:20 crosslinked sequencing gels containing 50% urea. Electrophoresis was carried out at 1000 volts for 7.5 h (381 bp fragment) or 4 h (167 and 517 bp fragments). Autoradiography was carried out at -70°C without the use of an intensification screen. An 8" x 10" copy of the original autoradiogram was scanned at 485 nm with the incident beam collimated to a width of 0.2 nm on a Cary 219 spectrophotometer. The data was recorded as absorbance relative to the film base density.

RESULTS

Footprints produced by partial cleavage of three DNA restriction fragments from plasmid pBR322 protected by Hoechst, netropsin and distamycin were examined. The 381-bp (Bam HI-Eco RI), 167 bp (Eco RI-Rsa I), and 517 bp (Eco RI-Rsa I) DNA fragments have several strong Hoechst, netropsin and distamycin binding sites. The DNA fragments labeled at the 5' (or 3') end with ^{32}P were allowed to equilibrate with Hoechst, netropsin and distamycin at ratios of ligand to DNA base pair of 0.06 and 0.03. Then MPE·Fe(II) was added to afford final ratio of MPE·Fe(II) to DNA base pair of 0.025. The reaction was initiated by the additon of dithiothreitol (DTT) at 4 mM concentrations. Cleavage by MPE·Fe(II) was stopped after 15 min (37°C) by freezing, lyophilization, and resuspension in a formamide buffer. The ^{32}P end-labeled DNA products were analyzed by high resolution denaturing gel electrophoresis capable of resolving DNA fragments differing in length by one nucleotide. The autoradiograms for MPE·Fe(II) footprinting on the 381, 167 and 517 bp fragments are shown in Figures 2.

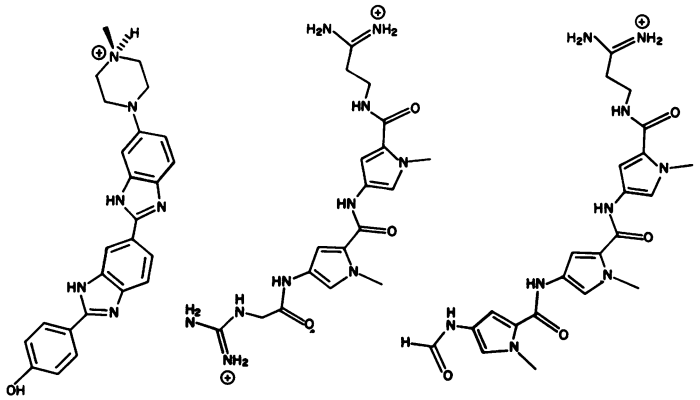

Figure 1. (Left to right) Hoechst 33258, netropsin and distamycin.


B
H H N N D D G
1 2 3 4 5 6 7 8 9 10 11 12 13 14 15 16 17 18
H H N N D D G

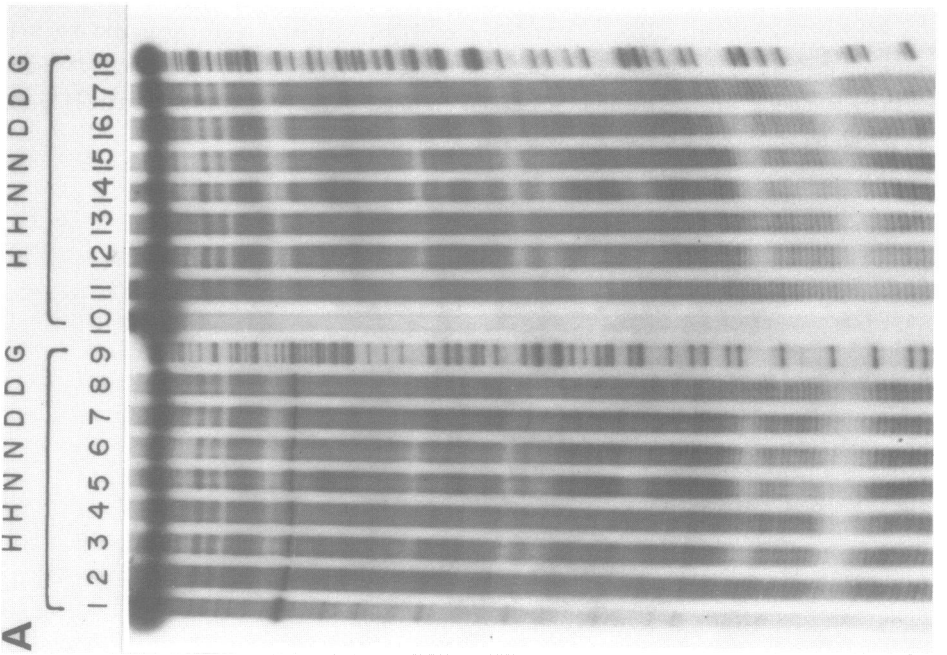
A
H H N N D D G
1 2 3 4 5 6 7 8 9 10 11 12 13 14 15 16 17 18
H H N N D D G

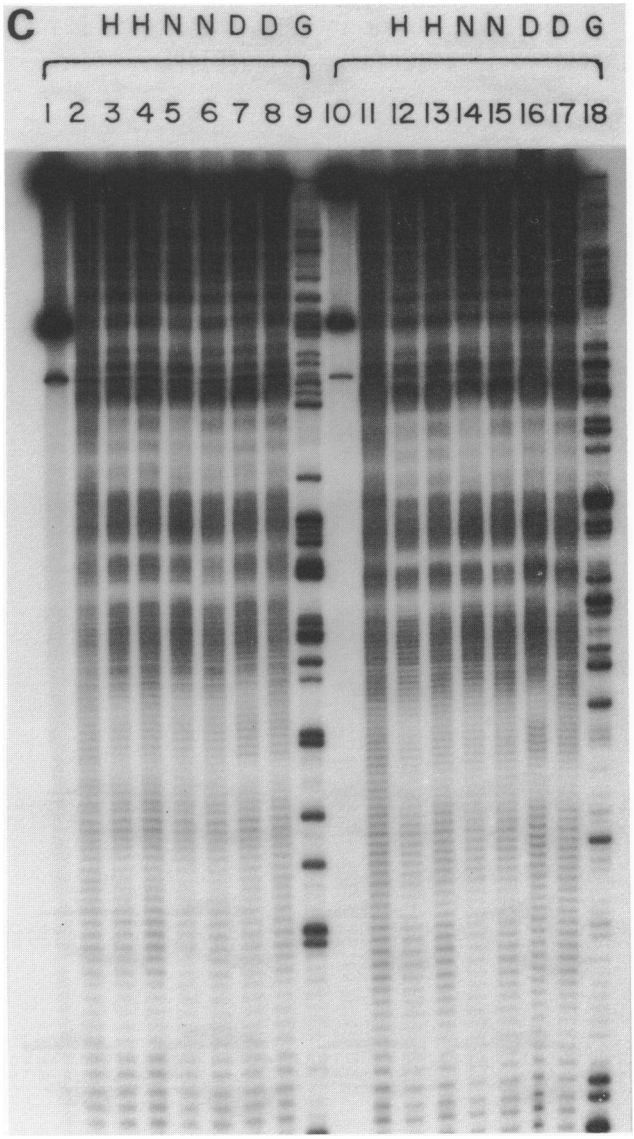

Figure 2. (A) Autoradiogram of 381 bp DNA restriction fragment, (B) 167 bp DNA restriction fragment, and (C) 517 bp DNA restriction fragment. Lanes 1-9 and 10-18 are DNA labeled with ^{32}P at the 5' and 3' ends, respectively, lanes 1 and 10, intact DNA; lanes 2 and 11, MPE·Fe(II) cleavage of unprotected DNA; lanes 3-8 and 12-17, MPE·Fe(II) footprinting with Hoechst at 6.3 μM (lanes 3 and 12) and 3.1 μM (lanes 4 and 13), netropsin at 6.3 μM (lanes 5 and 14), at 3.1 μM lanes (lanes 6 and 15) distamycin at 6.3 μM (lanes 7 and 16) at 3.1 μM (lanes 8 and 17); lanes 9 and 18 are the Maxam-Gilbert chemical sequencing G-specific reaction. Bottom to middle of the autoradiogram is the sequence left to right in Figure 3.

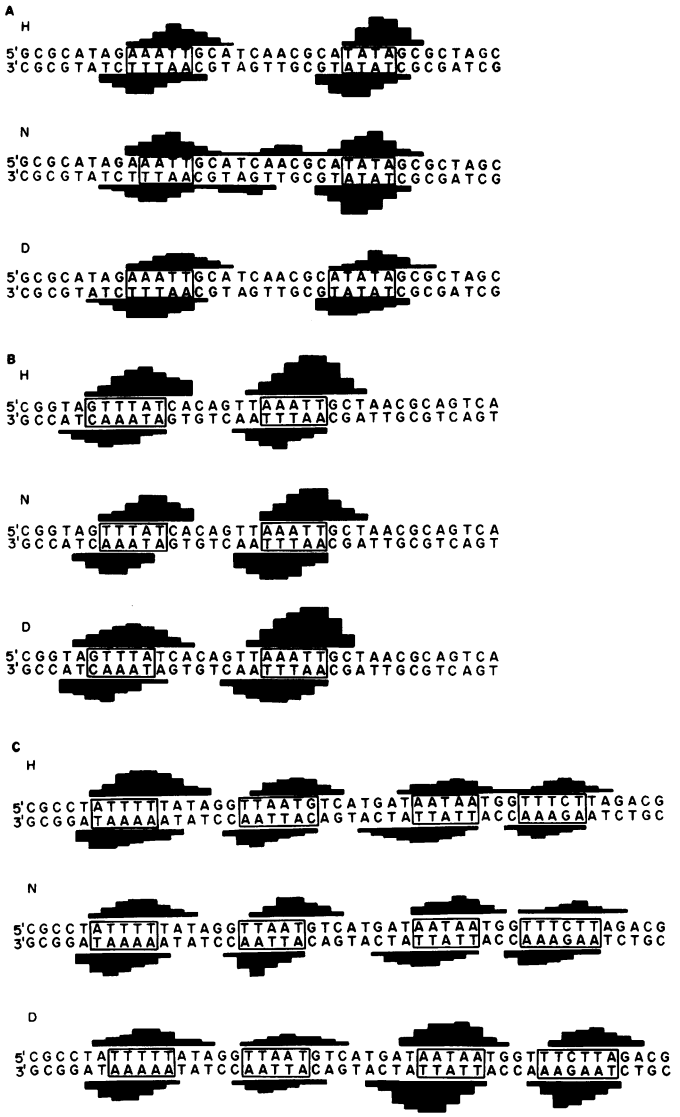

Figure 3. Footprints of Hoechst (H), netropsin (N) and distamycin (D) at 6.3 M concentration on (A) the 381 bp restriction fragments, bp 264-229 of pBR322 (Fig. 2), (B) the 167 bp restriction fragment bp 40-75 of pBR322 (Fig. 3) and (C) the 517 bp restriction fragment bp 4333-4286 of pBR322 (Fig. 4). The MPE·Fe(II) footprints (light regions in the gel autoradiogram, Fig. 2) are shown as histograms. The height is proportional to the reduction of cleavage at each nucleotide compared with MPE·Fe(II) cleavage of unprotected DNA (control lanes 2 and 11, Fig. 2). The top strand patterns are for 5' end-labeled DNA; the bottom strand patterns are for 3' end-labeled DNA. Boxes are the Hoechst, netropsin and distamycin binding sites, assigned by the asymmetric MPE·Fe(II) footprinting model (16,23,24).

Table 1. Binding Sites of Hoescht 33258 (H), Netropsin (N) and Distamycin (D)

Restriction Fragment		Binding Site	Site Size
381	H	AAATT	5
	N	aAATT	4
	D	AAATT	5
	H	aTATA	4
	N	aTATA	4
	D	ATATA	5
167	H	GTTTAT	6
	N	gTTTAT	5
	D	GTTTAt	5
	H	AAATT	5
	N	AAATT	5
	D	AAATT	5
517	H	ATTTTt	5
	N	ATTTTt	5
	D	aTTTTT	5
	H	TTAATG	6
	N	TTAATg	5
	D	TTAATg	5
	H	AATAA	5
	N	AATAA	5
	D	AATAA	5
	H	TTTCTta	5
	N	TTTCTTa	6
	D	tTTCTTA	6

Capital letters denote the sequence (5'-3') of the presumed binding sites. The lower case letters show the neighboring nucleotides.

The 381 bp Fragment (Bam HI-Eco RI). Control lanes 1 and 10 (Fig. 2A) are the buffered intact 381 bp restriction fragment of DNA (100 μM in base pair), labeled at the 5' (or 3') end with ^{32}P. Both denatured and renatured bands are seen in these lanes. Control lanes 2 and 11 (Fig. 2A) are MPE·Fe(II) cleavage of the 381-bp restriction fragment. Although a relatively uniform DNA cleavage pattern is observed, we note that MPE·Fe(II) cleavaged is not entirely sequence neutral and cleaves less efficiently at poly(dA·dT) regions. This is presumably due to lower affinity of MPE for A·T rich homopolymer tracts. Lanes 9 and 18 (Fig. 2A) are the Maxam-Gilbert chemical sequencing G reactions used as markers (22). Hoechst, netropsin and distamycin were allowed to equilibrate with the 381 bp DNA fragment at ratios of ligand to DNA base pair of 0.06 (Fig. 2A, lanes 3, 5, 7, 12, 14, 16) and 0.03 (Fig. 2A, lanes 4, 6, 8, 13, 15, 17) followed by partial cleavage with MPE·Fe(II). From densitometric analysis, the footprints

on 36 bp of the 381-bp DNA fragment are shown in Figure 3. MPE·Fe(II) cleavage reveals two common binding locations five ± one base pairs in size (Table I).

The 167-bp Fragment (Eco RI-Rsa I). Control lanes 1 and 10 (Fig. 2B) are the buffered intact 167-bp restriction fragment of DNA (100 μM in base pair) labeled at the 5' (or 3') end with ^{32}P. Both denatured and renatured bands are seen in these lanes. Control lanes 2 and 11 (Fig. 2B) are MPE·Fe(II) cleavage of the 167-bp restriction fragment. Although a relatively uniform cleavage pattern is observed, we note that MPE·Fe(II) cleavaged is not entirely sequence neutral and cleaves less efficiently at poly(dA·dT) regions. This is presumably due to lower affinity of MPE for A·T rich homopolymer tracts. Lanes 9 and 18 (Fig. 2B) are the chemical sequencing G reactions used as markers (22). Hoechst, netropsin, and distamycin were allowed to equilibrate with the 167-bp fragment at a ratio of ligand to DNA base pairs of 0.06 and 0.03 followed by partial cleavage with MPE·Fe(II) (Fig. 2). From densitometric analysis, the footprints on 36 bp of the 167 bp DNA fragment are shown in Figure 3. Cleavage with MPE·Fe(II) reveals two common binding locations five ± one base pairs in size (Table I).

The 517-bp Fragment (Eco RI-Rsa I). Control lanes 1 and 10 (Fig. 2C) are the buffered intact 517-bp restriction fragment of DNA (100 μM in base pair) labeled at the 5' (or 3') end with ^{32}P. Both denatured and renatured bands are seen in these lanes. Control lanes 2 and 11 are MPE·Fe(II) cleavage of the 517-bp restriction fragment. Although a relatively uniform DNA cleavage pattern is observed, we note that MPE·Fe(II) cleavaged is not entirely sequence neutral and cleaves less efficiently at poly(dA·dT) regions. This is presumably due to lower affinity of MPE for A·T rich homopolymer tracts. Lanes 9 and 18 are the chemical sequencing G reactions used as markers (22). Hoechst, netropsin, and distamycin were allowed to equilibrate with the 517-bp DNA fragment at a ratio of ligand to DNA base pairs of 0.06 and 0.03, followed by partial cleavage with MPE·Fe(II). From densitometric analysis the footprints on 48 bp of the 517 bp DNA fragment are shown in Figure 3. MPE·Fe(II) cleavage reveals four common binding locations five ± one base pairs in size (Table I).

DISCUSSION

Binding Locations and Site Sizes. Assignment of the DNA binding sites of Hoechst, netropsin and distamycin from MPE·Fe(II) footprinting is based on a model where the DNA cleavage protection patterns on opposite strands are asymmetric and shifted to the 3' side of the binding site (23,24). The most striking result visualized on the autoradiograms is that all three molecules bind common locations five ± one base pairs in size consisting mostly of A·T rich sequences on the three DNA restriction fragments (Fig. 2). The variation may simply reflect the inability of MPE·Fe(II) footprinting to resolve binding site sizes within one base pair. However, one base pair shifts in the maxima of the

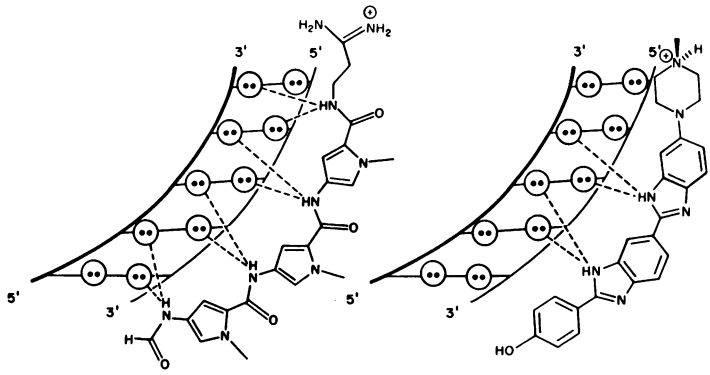

Figure 4. Model for distamycin and Hoechst 33258 in the minor groove of B-DNA. This is a refinement of the Mikhailov model (1) and is based on the X-ray structure of netropsin (14). Circles with two dots represent lone pairs of electrons on N3 of adenine and O2 of thymine at the edges of the base pairs on the floor of the minor groove of the DNA helix. Dotted lines are bridged hydrogen bonds to the bisbenzimidazole NH.

cleavage inhibition patterns from MPE·Fe(II) footprinting can be easily identified from the densitometric traces and are the basis for our assignments here. From affinity cleaving experiments on these same DNA restriction fragments, we know that distamycin has a binding site size of five base pairs (15-17). Distamycin binds these five base pair sites with two orientations (15-17). A footprint at a discrete location may be the sum of two orientations protecting that site. If both orientations bind the same base pairs, a minimum binding site size from footprinting will be observed. However, if the two orientations bind different bases within a common location, then the footprint from an MPE·Fe(II) cleavage experiment should be larger than the minimum binding site size.

Using MPE·Fe(II) footprints of distamycin as a guide, we find the maxima of the asymmetric inhibition patterns on opposite DNA strands are typically separated by one base pair. We assign the Hoechst and netropsin binding site size as five base pairs if the maxima of the asymmetric inhibition patterns are the same as distamycin, and four or six base pairs if the separation of the maxima is one base pair smaller or larger, respectively. Of the eight common binding locations analyzed on the three restriction fragments, Hoechst has a binding site size of five base pairs on 5 of the 8 sites, netropsin has a binding site size of five base pairs on 5 of the 8 sites and distamycin has a binding site size of five base pairs on 7 of the 8 sites (Table I). Although all binding sites for Hoechst, netropsin and distamycin are in common locations, not all sites are identical. The sites that are identical for all three molecules are (5'-3') AAATT and AATAA (Table I). At several locations there are variations of one to two base pairs. For example, on the 167 bp DNA fragment Hoechst, netropsin and distamycin bind (5'-3') GTTTAT, gTTTAT, and GTTTAt, respectively. On the 517 bp DNA fragment Hoechst, netropsin and distamycin

bind (5'-3') ATTTTt, ATTTTt, and aTTTTT, respectively, at one site, and TTTCTta, TTTCTTa, and tTTCTTA, at another (Fig. 3). Finally, we note that Hoechst, like netropsin and distamycin, will bind A•T rich sequences containing G•C base pairs (Table I) (2,16,17).

Molecular Origin of the Specificity of Hoechst. The MPE•Fe(II) footprinting data presented here reveals that Hoechst binds similar locations on DNA as netropsin and distamycin. If the specificity of these crescent shaped molecules for these common locations on DNA are of similar molecular origin, it may not be unreasonable to refine the Mikhailov model of Hoechst based on the crystal structure of netropsin bound to DNA (2,14). Similar to netropsin and distamycin, we presume that the binding of Hoechst to homopolymer A•T rich regions involves the displacement of water molecules in the spine of hydration (12,14). Like netropsin and distamycin, the electrostatic interaction of the cationic end and the negative potential in the minor groove of DNA undoubtedly contribute to the binding stability of Hoechst (13). From inspection of the models, Hoechst has two possible NH recognition elements on the bisbenzimidazoles capable of bridging adjacent adenine N3 or thymine O2 atoms on opposite helix strands in the minor groove of B-DNA. Therefore, based on the crystal structure for netropsin (14) and the n+1 rule for oligo-N-methylpyrrolecarboxamides (13-15), one might expect a binding site size for Hoechst of three base pairs due to bisbenzimidazole recognition alone. However, a binding site size of five ± one base pairs is observed. One possibility is that the Hoechst protection pattern on DNA results from more than one binding mode, such as two orientations that use some but not all common base pairs. The alternative explanation is that a single common central three base pair binding location is utilized by the bisbenzimidazole and in addition, the phenol and N-methylpiperazine rings flanking the bisbenzimidazole add a steric blockade of one base pair on each side of the A•T hydrogen binding site. This would afford overall protection from MPE•Fe(II) cleavage of five base pairs (Fig. 4). Similar to netropsin binding, perhaps Hoechst sits in the center of the minor groove with its four rings twisted noncoplanar, so that each ring is parallel to the walls of the groove to afford a good steric fit in the right-handed helix (Fig. 4). Why the binding by oligo-N-methylpyrrolecarboxamides and bisbenzimidazole in the minor groove of B-DNA helix is centered at the same locations must be due to the local micro-environment of these particular A•T rich sequences (Table I). Dickerson has pointed out that the sequence specific recognition of certain A•T rich regions may be the result of hydrophobic interactions in the minor groove and the NH hydrogen bonding elements simply align the inside edge of the crescent-shaped molecule on the floor of the minor groove of the helix (14). With regard to the design of synthetic sequence specific DNA binding molecules, a comparison of the Hoechst 33258, netropsin and distamycin structures suggests that flat aromatic rings twisted in a screw sense to match the walls of

the DNA helix and oriented on the floor of the helix by one or more bridged hydrogen bonds may be a general feature of B-form DNA recognition at A·T rich sequences.

ACKNOWLEDGEMENTS

Supported by the American Cancer Society research grant Number NP-428.

*To whom correspondence should be addressed

+Contribution no. 7162 from Division of Chemistry and Chemical Engineering, California Institute of Technology, Pasadena, CA 91125, USA

REFERENCES

1. Mikhailov, M. V., Zasedatelev, A. S., Krylov, A. S., & Gurskii, G. V. (1981) Mol. Biol. (Engl. Trans.) **15**, 541-553.
2. Martin, R. F., & Holmes, N. (1983) Nature **302**, 452-454.
3. Zimmer, Ch. "Progress in Nucleic Acids Research and Molecular Biology"; Cohn, W. E., Ed.; Academic Press: New York, 1975, p. 285-318.
4. Krey, A. K. "Progress in Molecular and Subcellular Biology"; Hahn, F. E., Ed.; Springer-Verlag: New York, 1980, Vol. 7, p. 43.
5. McGhee, J. D. (1976) Biopolymers **15**, 1345-1375.
6. Luck, G., Zimmer, Ch., Reinert, K. E., & Arcamone, F. (1977) Nucl. Acids Res. **4**, 2655-2670.
7. Patel, D. J., & Canuel, L. L. (1977) Proc. Natl. Acad. Sci., U.S.A. **74**, 5207-5211.
8. Berman, H. M., Neidle, S., Zimmer, Ch., & Thrum H. (1979) Biochem. Biophys. Acta **561**, 124-131.
9. Krylov, A. S.; Grokhovsky, S. L., Zasedatelev, A. S., Zhuze, A. L., Gursky, G. V., & Gottikh, B. P. (1979) Nucl. Acids Res. **6**, 289-304.
10. Van Dyke, M. W., Hertzberg, R. P., & Dervan, P. B. (1982) Proc. Natl. Acad. Sci., U.S.A. **79**, 5470-5474.
11. Gursky, G. V., Zasedatelev, A. L., Zhuze, A. L., Khorlin, A. A., Grokhovsky, S. L., Streltsov, S. A., Surovaya, A. N., Nikitin, S. M., Krylov, A. S., Retchinsky, V. O., Mikhailov, M. V., Beabealashvili, R. S., & Gottikh, B. P. (1982) Cold Spring Harbor Symp. Quant. Biol. **47**, 367-378.
12. Marky, L. A., Blumenfeld, K. S., & Breslauer, K. J. (1983) Nucl. Acids Res. **11**, 2857-2870.
13. Zakrzewska, K., Lavery, R., & Pullman, B. (1983) Nucl. Acids Res. **11**, 8825-8839.
14. Kopka, M. L., Yoon, C., Goodsell, D., Pjura, P., & Dickerson, R. E. (1985) Proc. Natl. Acad. Sci., USA **82**, 1376-1380.
15. Taylor, J. S., Schultz, P. G., & Dervan, P. B. (1984) Tetrahedron **40**, 457-465.
16. Schultz, P. G., & Dervan, P. B. (1984) Biomolecular Structure and Dynamics **1**, 1133-1147.
17. Youngquist, R. S., & Dervan, P. B. (1985) Proc. Natl. Acad. Sci., USA **82**, 2565-2569.
18. Van Dyke, M. W., & Dervan, P. B. (1983) Nucl. Acids Res. **11**, 5555-5567.
19. Van Dyke, M. W., & Dervan, P. B. (1984) Science **225**, 1122-1127.
20. Hertzberg, R. P., & Dervan, P. B. (1982) J. Am. Chem. Soc. **104**, 313-315.
21. Hertzberg, R. P., & Dervan, P. B. (1984) Biochemistry **23**, 3934-3945.
22. Maxam, A. M., & Gilbert, W. (1980) Method Enzymol. **65**, 499-560.
23. Van Dyke, M. W., & Dervan, P. B. (1983) Cold Spring Harbor Symposium **47**, 347-353.
24. Van Dyke, M. W., & Dervan, P. B. (1983) Biochemistry **22**, 2373-2377.